Development of an in-line Production Quality Assessment System for Thin Film Devices

Isaac Kwasi Yankey

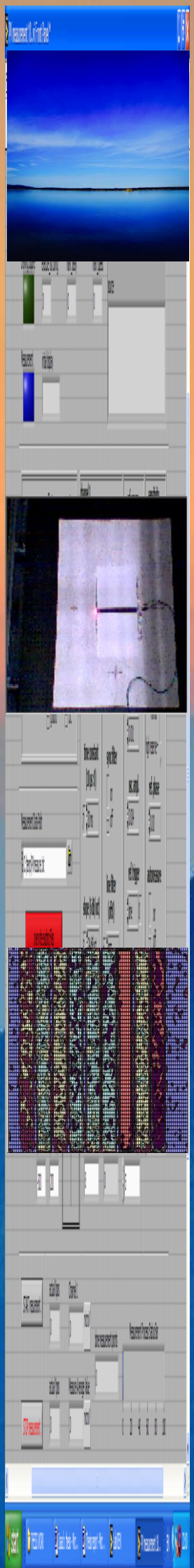

Publishing Partner:
IJSRP Inc.
www.ijsrp.org

Publication Partner:
International Journal of Scientific and Research Publications (ISSN: 2250-3153)

Development of an in-line production quality assessment system for thin film devices

Isaac Kwasi Yankey

Publishing Partner: IJSRP Inc.

ISSN 2250-3153

9 772250 315302

Copyright and Trademarks

Preface

The interest in green and clean energy has increased significantly in recent years. Also, due to fossil fuel economics and spent fuel handling associated with nuclear power, renewable energy will play a major role in meeting the world's energy demand. Due to global warming, ozone depletion and other environmental concerns, the replacement technology is likely to be one free of strings like solar photovoltaic power, which produces very little pollution during its operation.

Several challenges present themselves when developing thin-film materials for large scale applications. While research on solar cells have achieved efficiencies comparable to single crystal silicon material, issues such as local defects and overall uniformity become increasingly important as the deposition area is increased. A technique for detecting such problems will be of great importance to the solar cell industry. Moreover, valuable information could be deduced from mapping the spatial distribution of localised properties of solar cells.

A laser beam induced current measurement (LBIC) technique is used to explore the effect of non-uniformity and defects in devices in the early part of the production stage and help explain lower efficiencies in certain types of solar cells. The equipment construction and the control system used to take measurements for analysis is viewed with the overall goal in mind: as a tool for assessing the homogeneity of thin film deposition, spatial variation of diode characteristics and local defects on device performance with the idea of improving production quality assessment system and hence the cell efficiency of economically viable solar cells.

This monograph serves as an excellent academic resource for Technicians, undergraduate and postgraduate students in the Renewable Energy Sector. Also, a good reference material for use by energy investors interested in the Solar Photovoltaic, Manufacturing companies in the solar industry, Control Engineers and Electric Utility Companies.

ACKNOWLEDGEMENT

I am indebted to Dr. Ralph Gottschalg my supervisor at Loughborough University (CREST) and Dr. Andrew Martin, Department of energy technology (KTH) for their invaluable suggestions, constructive criticisms and critical reading of this research. I also express my appreciation and gratitude to Mr. Martin Bliss for his tremendous help in programming the system. A great thank you to Dr. Tom Betts and Sheryl Williams for spending time to read this work and their suggestions and discussions. I further express my gratitude to the senior members and fellow students at CREST and Department of energy technology (KTH), especially Emmanuel Doro, Jerret Chinedu, Isaac Kwaku Adu, Mathew Little, Rupert Gammon and others who in diverse ways contributed to the success of this research. My appreciation goes to all friends especially Mr Clement Aboagye-Ampah, Edward Kwame Obese and George Effah and his wife for their support.

I extend my sincere gratitude to my brothers: Mr Abdul-Rahman Yankey, Mr Moses Yankey and his wife and, my sisters: Grace Dadzie, Dorothy Yankey, all my in-laws, sons and daughters who always supported me financially and morally in my studies.

Above all, I thank the almighty God for his guidance through out the study.

Author

Isaac Kwasi Yankey

Department of Energy Systems Engineering, (KTU)

Mr Isaac Kwasi Yankey is currently a lecturer at the Department of Energy Systems Engineering at Koforidua Technical University in Ghana. At University of Cape Coast, he studied Physics and earned a Bachelor of Science honours degree in 1999. He studied Master of Science (MSc) in Mechanical Engineering (Sustainable Energy Engineering) at Royal Institute of Technology- Sweden in 2004 and another Master of Science (MSc) degree in Project Planning and Management at University of Bradford-United Kingdom in 2007. He is part of a team of researchers working on the Renewable Energy Technology Transfer for Ghana Energy Commission and UNDP from 2016 to present. Also, a member of the research team participated in the SOLtrain West Africa Program for Ecowas Centre for Renewable Energy and Energy Efficiency (ECREEE) since 2015 to date. Currently a liaison coordinator for the Department of Energy Systems Engineering at the Koforidua Technical University in Ghana.

TABLE OF CONTENT

INDEX OF FIGURES

NOMENCLATURE

Physical Constants

q	Electronic charge	$=1.602\text{x}10^{-19}$ coulomb
k	Boltzmann's constant	$=1.380\text{x}10^{-23}$ joule/K
$\frac{kT}{q}$	Thermal voltage	=0.02586V (at 300K)
AM0	Air Mass Zero	$=1353\text{kW/m}^2$

List of symbols

λ	Wavelength of light
A	Cross sectional area
C	Speed of light
G	Global irradiance
h	Plank constant
I	Current
I_o	Diode saturation current
I_D	Diode current
I_L	Load current
I_{MP}	current in the maximum power point
I_{PH}	Photogenerated current
I_{SC}	Short-circuit current
N	Number of photons
R	Resistance
R_L	External load
V	Voltage
V_{MP}	Voltage in the maximum power point
V_{OC}	Open-circuit voltage

CHAPTER ONE

BACKGROUND

1.1 Introduction

Renewable energy systems are an integral part of today's and future sustainable energy scenarios. Various energy options must be provided to meet the world's exponentially growing population and the demand for high standard of living. The dwindling reserves of fossil fuels are leading to global demand for a new source of power. The interest in green and clean energy has increased significantly in recent years. Also due to fossil fuel economics and spent fuel handling associated with nuclear power, renewable energy will play a major role in meeting the world's energy demand. Due to global warming, ozone depletion and other environmental concerns, the replacement technology is likely to be one free of strings like solar photovoltaic power, which produces very little pollution during its fabrication. Also very little pollution while in use and at the end of its lifecycle if a reuse/recycling programme is implemented.

Wind, hydro, solar and geothermal energy are a few of the renewable energy sources that exist. Solar power, especially photovoltaics is one of the renewable energy resources with the potential of meeting a significant percentage of the worlds energy demand. Although some types of photovoltaic have reached a market status, there is still extensive research and development on novel designs. Energy produced from photovoltaic is current used for powering watches, calculators and remote housing. A major drawback of photovoltaics is its low efficiency of cells and modules. For this energy resource to have a significant influence on the world's energy market, higher efficiencies are needed for grid connection. Currently, the cost of power generation from photovoltaic is much higher than power from fossil fuel, and PV being a new technology must be able to achieve less than 1€/W with a multi-GW/yr [Michel, 2004] manufacturing rate to be able to compete with conventional fuels.

There are three main types of solar cells on the market. These are polycrystalline, thin-film and monocrystalline. Each of these solar cells has its own merits and

demerits with thin films being theoretically inexpensive but low efficiencies. Moreover, thin-film efficiency has been improving over the years by improving the quality of manufacturing methods.

Solar cells based on thin-film technology may provide much of the answers to give inexpensive, widely available solar energy. With high speed, large area deposition of semiconductor materials on glass or other substrates, some sacrifice in efficiency compared to single-crystal technologies will likely be made. However, efficiencies nearly 20% [Schultz el. al, 2004] have been demonstrated and the lower cost of materials promises lower end prices for the consumer.

Several challenges present themselves when developing thin-film materials for large scale applications. While research on cells have achieved efficiencies comparable to single crystal silicon material, issues such as local defects and overall uniformity become increasingly important as the deposition area is increased. In addition, performing research on some thin film solar cells is not always straight forward because of the interactions between different layers of the solar cell. A technique for detecting such problems will be of great importance to the solar cell industry. Moreover, valuable information could be deduced from mapping the spatial distribution of localised properties of solar cells.

The aims of this research follow from the fact that electrical measurements and production quality assessment are usually performed on finished devices and characterise the entire area of the cell as a whole. A laser beam induced current measurement (LBIC) technique will help explore the effect of non-uniformity and defects in devices in the early part of the production stage and help explain lower efficiencies in certain types of solar cells. The equipment construction and the control system used to take measurements for analysis should be viewed with the overall goal in mind: as a tool for assessing the homogeneity of thin film deposition, spatial variation of diode characteristics and local defects on device performance with the idea of improving production quality assessment system and hence the cell efficiency of economically viable solar cells.

The basic principle underlining laser beam induced current measurement technique is to focus a laser beam onto a photosensitive surface such as solar cells and the generated short circuit current measured. This measured current can be used to draw a map of the of the cell surface which can then be used in investigating structural defects in the cell. Defects can be diagnosed and the process in manufacturing causing it and thereby possibly improve production techniques for homogenous thin-films and hence improved cell performance and efficiency.

The next part of this work will focus on the literature review of existing techniques and theory of thin films with a more detailed review of laser beam induced current principles. Chapter 3 contains information on the laboratory facility, including the control mechanism employed, devices communication, instrument drivers and the software used in this system. Testing of the system and results on this modelling was discussed. This work finished with a chapter on the overall summary, conclusion and recommendation of the future work that should be done.

CHAPTER TWO

RELATED LITERATURE

A short overview of properties relevant to this work of solar cells is given. Light absorption by semiconductors and electrical characterisation are introduced and a brief overview of the operating principles of an LBIC is given.

2.1 Thin film solar cells

Solar cells can be made from thin films of various materials into different types. The types of thin films which have emerged to be of likely commercial importance are Amorphous silicon (a-si), copper indium diselenide (CIS) or copper indium gallium diselenide (CIGS) and cadmium telluride (CdTe). Some of these materials are made up of p-type absorbers with bandgaps well matched to the solar spectrum [Markvart, 1997] (~1.5 and ~1.15 eV).

Amorphous silicon has a bandgap of 1.75 eV and is more strongly absorber of light. This property of strong light absorber and several other properties such as silicon, a familiar and plentiful material and a method that could be employed to make uniform large area modules made it more desirable as a thin film material. Aside these positive signs are the problems of spatial inhomogeity, dangling bonds and other defects. But the technology to demonstrate high efficiency, a-si modules awaits more advance production technique. Therefore, LBIC technique has the capabilities of analysing and detecting defective cells in the production line. A figure illustrating the structure of amorphous silicon is shown below.

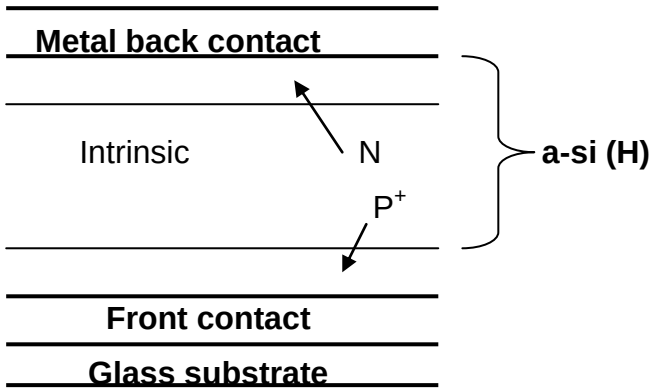

Fig 2.1 Schematic diagram illustrating major structures of an amorphous silicon PV cell. [Markvart, 1997]

2.2 Absorption of Light

The entire technology of PV cells is based on the use of sunlight by solar cells. Solar cells absorb sunlight and convert it directly to clean electricity that is sustainable and environmentally friendly. The "fuel" for PV is therefore solar radiation, which amounts to about 4.4 $X10^{17}$ [Markvart 1997] on the Earths surface. Mobile charge particles are created when incident energy of light hits a photosensitive surface. This is due to the quantum nature of light, which is perceived as a flux of particles called *photon* with an energy given as;

$$E_{ph} = \frac{hc}{\lambda} \qquad 2.1$$

Where *h, c and* λ Planck's constant, speed of light and wavelength of light respectively. The amount of striking photons on the earth surface per square centimetre is about 4.4x 10^{17}. [Markvart 1997]. Only those with energy in excess of the band gap can be converted by the solar cell into electricity.

When a photon with this amount of energy enters a semiconductor, it is absorbed and increases the electron energy in the valence band. This increased energy allows the electron to jump from the valence band to the conduction band there by creating a *hole* in the valence and an excess electron in the conduction band. Hence and *electron-hole* pair is generated.

The electric current that such photons can generate i.e. can be estimated with equation 2.2 if fundamental losses are neglected. [Markvart 1997]

$$I_{\lambda} = qNA \qquad 2.2$$

It is clear that the generation of electron-hole pair also creates excess energy since the promoted electron has energy higher than the band gap. This energy is dissipated in the semiconductor in a form of heat and is not useful for electricity production and forms one of the fundamental losses in solar cells.

2.3 Electrical Characterisation of Solar Cells

A solar cell is a semiconductor diode and its operation is primarily the conversion of sunlight into electrical energy by the process of photovoltaic effect. Incident energy of light produces electron-hole pair by the interaction of the incident photon with the atoms of the cell. The electric field created by the cell junction causes the photo-generated electron-hole pairs to be separated. This separation occurs through the movement of electrons into the **N**-region of the cell and holes drifting into the **P**-region. This is achieved by fusing semiconductor material with different electronic characteristics to form a junction. Electricity can then be generated under this circumstance when the surface is illuminated.

Figure 2.2 shows an equivalent circuit that may be used to model the behaviour of a solar cell.

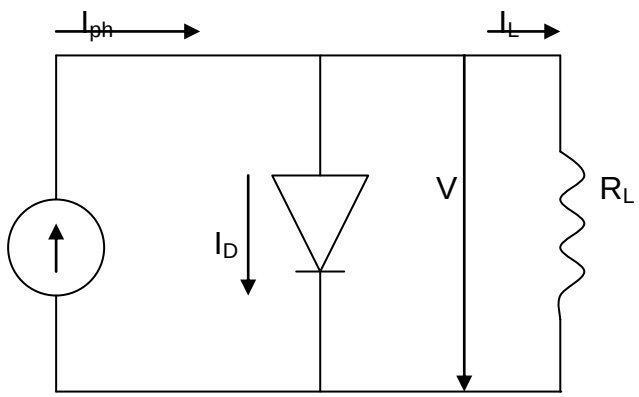

Fig 2.2. Equivalent circuit diagram of a solar cell.

In this figure R_L represent the external load and the voltage across the load and the current through the load as V and I_L respectively.

Two quantities of interest for a solar cell are the following: short circuit current (I_{SC}) and open circuit voltage (V_{OC}). When the cell is connected in a short circuit with nearly resistance-less wire, the current measured is called the short circuit current and when the circuit is opened the voltage across the diode and the load is called the opened circuit voltage. These are the two parameters used to characterise the output of a solar cell at a given irradiance, temperature and area.

In an ideal case the I-V characteristics of a cell is given as:

$$I = I_l - I_o\left[\exp\left(\frac{qV}{nKT}\right) - 1\right] \qquad 2.3$$

Where I , is the current, V the voltage, q electron charge, K Boltzmann constant, T is the absolute temperature, I_l is the load current and I_o is the diode saturation current.

To determine the short circuit current of the PV cell, V is set to zero:

$$I_{sc} = I_l \qquad 2.4$$

Hence to a good approximation the cell current is directly proportional to the available sunlight.

To determine the open circuit voltage (Voc) of the cell, the cell current is set to zero in equation 2.3 which yields,

$$V_{OC} = \frac{nKT}{q}\ln\left(\frac{I_{SC}}{I_o} + 1\right) \qquad 2.5$$

The open circuit voltage is logarithmically dependent on the cell illumination.

I-V characteristics curve of a solar cell is obtained by plotting the output current as a function of the output voltage. This can be achieved experimentally by varying of the load from zero ohms to several kilo-ohms while the cell is illuminated. The curve generated is in the fourth quadrant indicating that power is being supply to the load and an absolute values reflects the curve into the first quadrant as shown in figure 2.3.

Figure 2.3 and 2.4 shows a real I-V and P-V curves respectively of a-si at STC provided by Vorasayan [2004]

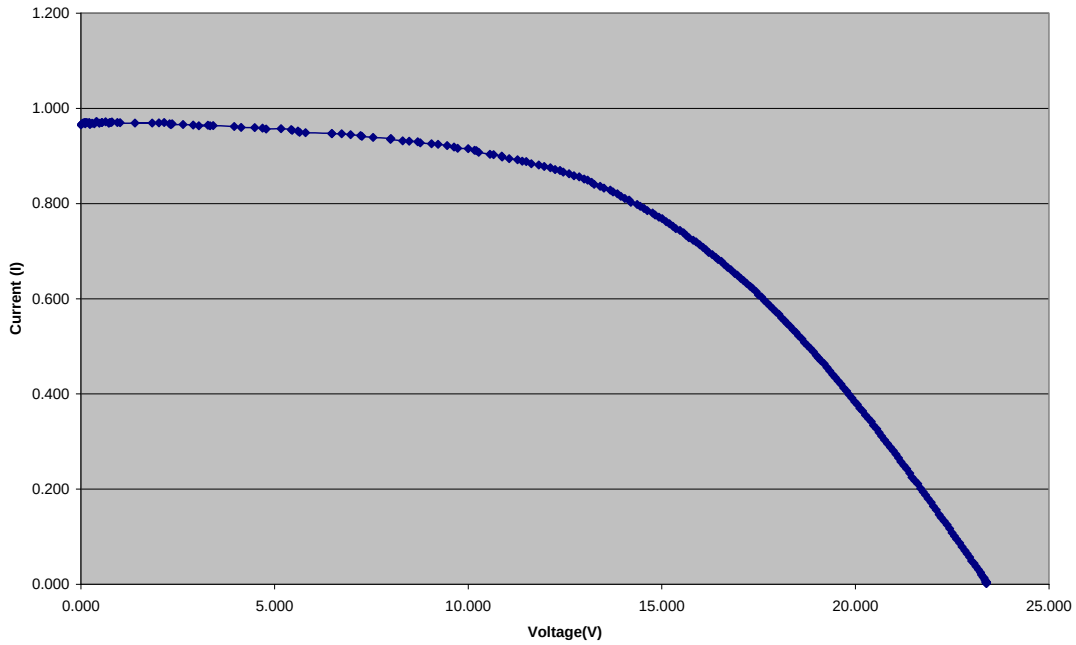

Fig. 2.3 I-V characteristics curve of a PV module (Source: Vorasayan 2004)

The cell voltage multiplied by the cell current yields the cell power. With the idea of optimising the performance of (costly) PV module, it is desirable to operate the cell at maximum power; there is one point on the I-V curve where this maximum power occurs. This maximum power can also be found by plotting the cell power versus voltage as shown in figure 2.4

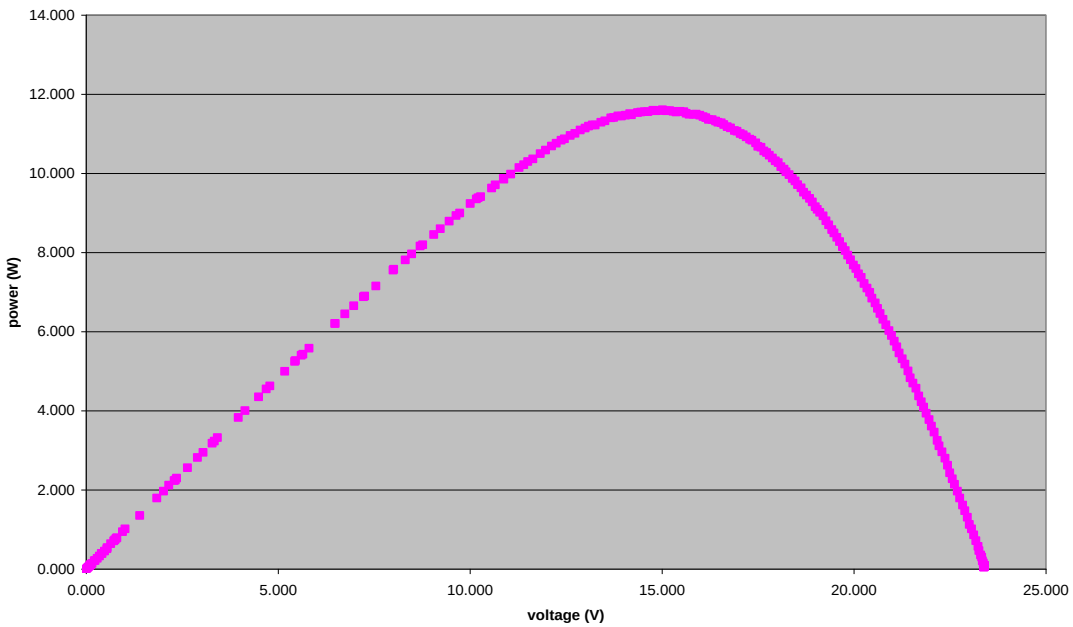

Fig.2.4. P-V curve of a PV module (source: Vorasayan 2004)

Therefore, cells and modules are designed to produce electricity, when they are near their maximum power. Hence the maximum power can never be equal to the product of the open circuit voltage and the short circuit current; hence the closeness with which the maximum power approaches this product is called the ***Fill Factor***.

The fill factor is given as:

$$FF = \frac{I_{MP} \times V_{MP}}{I_{SC} \times V_{OC}} \qquad 2.6$$

Where I_{MP} is current at maximum power point and V_{MP} is voltage at maximum power point. Amorphous silicon has a fill factor value of 0.7. [Michel 2004]

2.4 Laser Beam Induced Current principles.

Laser beam induced current (LBIC) is one of the techniques which has been developed to analyse in-line production quality of solar cells. This technique has been used in other laboratories and is quite straightforward. The basic principle underlining this method is as follows: a sample solar cell or a photosensitive device is illuminated by a laser source with an appropriate spot size, and the generated current or voltage is measured either by a lock-in amplifier or other device required by the set-up [Michel 2004]. Topography of the sample's current can be mapped by either moving the

sample or the laser source. With the recorded mapping, defects can be traced and affordable quality control will be in the production line for mass production to reduce cost and increase practical efficiency. The collected photocurrent probes the spatial variations in the device, including the local quality of the junction, spatial variations in the resistivity and local shunting effects. Additional data processing yields information directly applicable to the question of quality assessment, uniformity and local defects.

Similar techniques have been applied to different types of polycrystalline silicon devices which have grain sizes typically 100 times greater than those in polycrystalline CdTe and CIGS materials [e.g. see Acciarri et al, 1996], [Rezek et.al, 2002], [Acciarri, 2002], [Dunlop, et al 1997]. In addition to addressing the uniformity and current mapping of solar cells, researchers have the means to extract device parameters related to carrier dynamics, such as minority carrier diffusion length, with measurements of the response near grain boundaries. But because of the much smaller grain sizes and other concerns specific to thin film devices one cannot apply all these analyses to thin film solar cells.

The apparatus under investigation in this research will provide a unique characterisation of the uniformity of collection efficiency and current mapping of multiple cells. The basic components involved in such a system are the following: a laser source for generating electron hole pair; a device for measuring the generated signal (Lock-in amplifier); an optical chopper which intercepts the laser beam on a periodic basis; and a computer to display, analyse and control the system. The optical chopper is used to chop the laser beam and the reference output is used to lock the lock in amplifier to the chopped frequency. Since the light source is monochromatic and cannot be modulated electrically, one must chop the light to use phase sensitive detection. A lock-in amplifier in it most basic form is an instrument with dual capabilities. That is it can recover signal in the presence of overwhelming noise background and also provide a high-resolution measurements of several orders of magnitude and frequency. A detailed description of the Lock-in amplifier is given in the next chapter. Several researchers and laboratories have used LBIC techniques to

investigate thin-film polycrystalline deposited material [Delahoy, 1997], [McMahon, 1997] and post deposition treatments. [Galloway, 1995]

The method used by Galloway differs from the current LBIC experimental technique because it is based on a scanning electron microscope to produce current maps from the interaction between a high energy electron beams with the atoms in the sample surface. This method becomes more difficult as the junction depth increases and the complexity of the structures increases.

Also more general uniformity investigation and detection of junction failures has been done with high speed and large area scanning methods. [Acciarri et al, 1996], [Rezek et.al, 2002], [Acciarri, 2002], [Dunlop, et al 1997]

The system differs from other system base on the fact that is very fast scan and also unique for amorphous silicon due to the fact that quantum efficiency of amorphous is best at this laser frequency. Also the current system can scan up to 1.2 X 1.2m module which is a standard size for commercial cells.

Every LBIC system is unique to the experimental aims and ranges from simple set-ups to complex ones with triple laser scanning spots and multiple Lock-in amplifiers. The multiple uses of lasers enable easy separation of the photocurrent components and also to achieve a larger spot size based on the application and the need for highly detailed maps. Reflection measurements of the sample are achieved when a multiple Lock-in amplifiers are used [Kress et al]. A detail description of the LBIC technique used in this work will be given in the next chapter.

CHAPTER THREE

EXPERIMENTAL SET UP

3.1 Introduction

This chapter provides a detailed description of the experimental set up of the LBIC system used in this work. Also, the communication protocols used in controlling various instruments and the software interface are described.

3.2 Operational Principles

The basic components of this set-up consist of the following;

- A laser source: The incidence of laser light onto this cell with a specific frequency is used as a tool to give more insight into the cell behaviour. The test sample is illuminated with a Helium-Neon (HeNe) laser with a wavelength of 635nm. The number of electrons released in a photocell per photon of incident radiation of specified wavelength is high for a-si in a wavelength range between 600-650nm and hence HeNe was chosen base on the quantum of efficiency of amorphous silicon.
- An optical system for guiding the laser across the sample: The focusing of the laser is done by varioSCAN 20 which is in front of the scan head and the movement of the laser over the sample surface in an X-Y direction is achieved by two deflecting mirrors (ScanLab, SCANgine14) with the help of two tilted galvanometric mirrors. Both the scan head and the dynamic focusing system are controlled through a PC via a special user interface board (RTC-3). This is a 3-D scanning system because of its capability to focus the beam onto the working plane.
- Measurement equipment: The core of the measurement system is the lock-in amplifier. The two basic functions of the lock-in is signal recovery in the presence overwhelming noise and provide high resolution measurements of clean signals over several magnitude and frequency. A special rectifier called phase-sensitive detector (demodulator) converts AC signals to DC by multiplying two signals together and is the heart of the lock-in Amplifier. In real world situation signals are accompanied by noise. This noise by definition

has no fixed frequency or phase relationship to the reference. The demodulator then singles out the component of the signal at a specific reference frequency set by the optical chopper in this case and suppresses the effect of the accompanied noise. Noise components at frequencies close to that of the reference may result in demodulator output but by setting the low-pass filter to low cut-off frequency; these can be rejected. Therefore, a combination of low pass out filters and phase-sensitive detector allow small signals to be measured in the presence of significant noise.

- A physical structure for mounting the equipment: A framework of aluminium extrusion contains the laser and the working space (1.2x1.2m) which provide vibration free platform for the system. The encasement allows the system to be classified as Class I laser. On top of the aluminium frame is a small breadboard that serve as a platform for the laser, the chopper and the optical guidance and the laser and the optical devices are fixed at about 2m above the working surface. The doors have locks to enforce security and are electronically connected such that, the laser is cut-off when the doors are opened. The background is illuminated by 108 halogen lamps mounted underneath the laser platform to allow operating conditions close to a solar simulator. The alignment of the halogen lamps are such that the in-homogeneity is about 5% and the measured irradiance on the work surface is 315 $W/m^2 \pm 4\%$.[Michels, 2004]
- Software for instrument control and acquisition of data. The detail of the software interface has been treated in the next section.

A further description of each of these components has been given previously by Michel, 2004 and a diagram showing the set-up with dimensions of (1.2 x1.2 X 2m) is shown below.

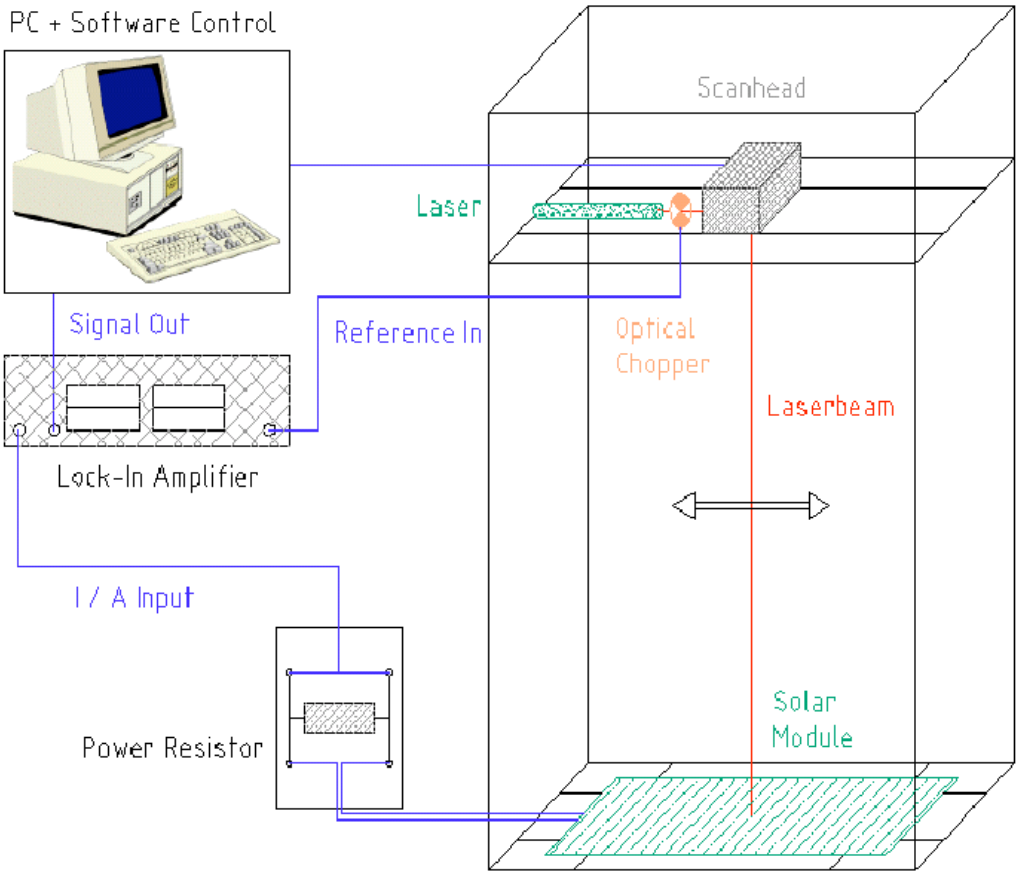

Fig 3.1 Experimental set-up of LBIC system (Source: Michels, 2004)

In this system a focused laser is made to strike onto the surface of a solar cell mounted in an XY plane which allows the laser to scan its surface. With an optical system guiding the laser beam over the photosensitive surface, photocurrent topography of the whole cell/module can be mapped and a 3D graph can be drawn for fault detection and analysis of the device. The data is then stored in an array format and saved to file as current generation as a function of laser position. The range of module sizes that are produced by companies is important in determining the scanning area of the LBIC system. Currently, the set up can scan a module size of ca. 1.2m x1.2 m [Michels, 2004].

The whole scanning and data acquisition system was originally programmed in Delphi. However, this system had its problems and it was decided to re-work this in LabVIEW (Laboratory Virtual Instrumentation and Engineering Workbench programme by National Instruments) as part of this work.

3.3 Instrument Control

Today, a vast array of devices, software and techniques are available for instrument control. The development of digital signal processing enables the required information to be obtained from a sensor and presented in an appropriate form. This has increased the range and diversity of modern instrumentation. National Instruments' LabVIEW software was used to communicate with and control the external instruments such as the movement of the laser beam and the lock-in amplifier. The laser and its optical components are controlled through an RTC 3 board through direct link library (DLL). The DLL contains the commands to communicate with the RTC 3 board. This interface board is design for real time control of scan heads and lasers with a PC bus interface. The implementation of the control routine of the DLL was achieved through the call function library in LabVIEW. A call function library in LabVIEW converted the Visual Basic programming language that communicates with the RTC3 interface into a graphical language that LabVIEW understands. It contains the commands and instructions used to control the movement of the deflecting mirrors and the focusing of the laser beam onto the cell. The parameters for the X-Y coordinates are as signed 16-bit values. Data transfer and control is done through General Purpose Interface Bus. This is a standard bus use for controlling and interconnecting measurement devices. The control and communication between instruments was achieved through intuitive ASCII commands.

3.3.1 Communication Interface

The board which is currently being used has already been installed, configured and programmed to take measurements in a Borland DELPHI scripted program, but communication with the amplifier had been identified as a problem, introducing long delays in the measurement cycle [Michel, 2004].

In trying to solve this problem, a lock-in amplifier driver software from National Instruments was used to programme the lock-in amplifier in order to ensure compatibility. Before communication can be established, the connected instruments in the set up must be detected. This was done with ***Measurement & Automation***

Explorer (MAX) in Labview. This automatically identifies the connected instruments, installs the necessary instrument drivers and manages the instrument drivers already installed. The MAX configuration was used to locate the instruments, by their primary addresses, the names of the instruments, the GPIB interface number that was used to configure the board and the description of the attached instrument. The GPIB interface board representation in MAX and the results of scanning for instruments (button at the top left of the MAX window) is shown in the appendix. By default, the GPIB board is always given an address 0. This has been shown in the appendix.

The Instrument I/O VI was used to test the communication flow among the instruments identified in the Measurement and Automation Explorer. This improvement was due to the fact that IEEE 488.2 driver was created for the GPIB board and this established the readiness of the instruments to make measurements using the command **query and paste** which establish detail information about the connected devices which is the lock-in amplifier. This yields a series of the instruments by naming them as TOKEN 0, 1, 2, etc. Each of these commands gives specific information about the lock-in amplifier and is illustrated in the figure below. After the initialisation of the communication channel to an instrument, it is necessary to know the resource name or descriptor.
For example, **GPIB::8::INSTR** is the instrument descriptor for the GPIB instrument at address 8 and in this case is the lock-in amplifier in the LabVIEW Graphical Programming language.

3.3.2 Instrument Drivers.

The instrument I/O functions can communicate with the driver-level software of the GPIB board and hence VIs can be built using these command functions. Different instruments have different specific sets of commands and communication protocols for sending and receiving data. Learning these low level commands for each instrument is time consuming and difficult. Hence instrument drivers save time by eliminating the need to learn complex low-level programming commands for each of the instruments in the set up.

An instrument driver is set of software functions or VIs that use the instrument commands or protocol in performing common operations with the instrument. [Wells, 2000] The following are typical for instrument drivers:

- Receive, Parse and scale the response into scaled data that can be used for test applications.
- Call on the appropriate functions and VIs for the instrument.
- Instrument drivers have VIs in the following Categories: **initialise configuration, action/status, data and close.**

The GPIB board used in the set up is not a National Instruments card but the software interface is, and therefore it was necessary to create an AT-GPIB/TNT driver. This enabled LabVIEW to recognise the board as if it was from National Instruments and communicated perfectly with it through MAX, although there is some limitation on how far commands can be used in MAX. The driver for the peripheral equipment (in this case the lock-in amplifier) was another vital piece of software that was needed for instrument control in LabVIEW. A driver palette for the lock-in amplifier SR830 that was created in LabVIEW is shown (Appendix).

3.3.3 Software Interface

The software used in programming the current system is written in LabVIEW which is from National Instruments. This is a fast and less tedious application development language for controlling instruments.

The application is started by launching the LabVIEW programme from the desktop or pressing the start button. The main window which appears after starting the program contains the front panel toolbar and buttons for controlling the laser movement by first initialising the laser, starting and stopping measurements. The software by default has a run and stop button on the top left of the window and controls the overall measurement and data acquisition and these buttons are started first before the sector buttons in the application. The front panel of the lock-in amplifier has been programmed in the software and can be controlled by the software instead of manual controls on the amplifier itself.

A status bar which shows how the measurement is progressing and the percentage of points measured is also indicated and with the help of the error codes, measurements can be stopped or continued. The data is stored in an array format in the application and then saved to file in an excel format and hence graphing and analysis are carried out in excel.

The software contains several fields to type in parameters for the measurement set up such as: number of measurement points, steps taken in X and Y directions, the number of repeated measurements taken at each point. This has an influence on the total time taken to measure the whole module.

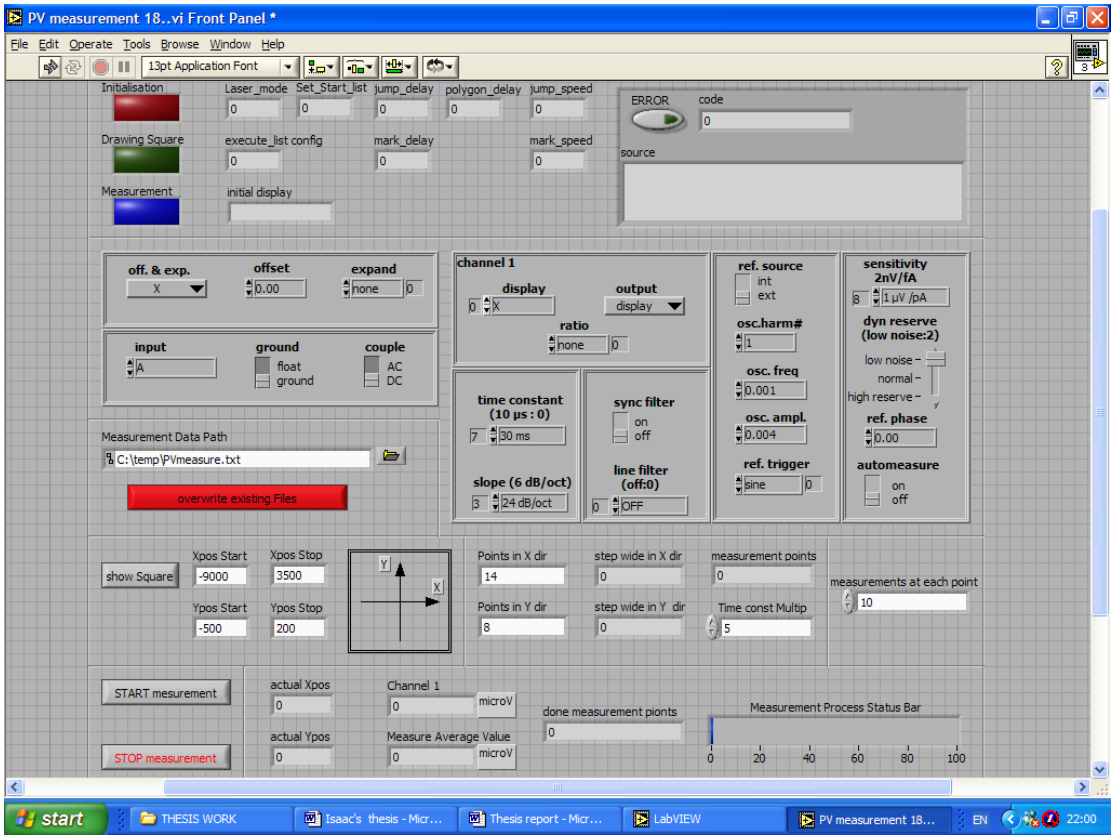

Fig 3.2 Main window of the software programme.

Behind this window (Fig 3.2) lies the block diagram which holds the programming codes for the application and is made up of sub VIs and VISA command. VISA is a high level communication protocol that LabVIEW uses and it has been used in developing this application.

CHAPTER FOUR

MEASUREMENT AND ANALYSIS

4.1 Introduction

Several settings are available and possible to change before the measurement process begins. These settings, such as time constant, gain, sensitivity and line filters on the lock-in amplifier have an influence on the results of the output current which is sent to the computer. Interacting with the user interface of the lock-in amplifier, settings that can be varied for better and higher resolution mapping are varied through the software application. This chapter explains these variable settings and their influence on the spatial resolution and data quality of the application.

4.2 Testing the control system

A flow chart showing how the current LBIC system works is shown in fig 4. This has four main steps as illustrated in the chart: *initialisation of the laser, the input data, the measurement process and the output data.* These are the four main parts of the software to monitor and control the scanning process for one measurement cycle.

The first stage through the control system is the initialisation of the laser which currently has been programmed to initialise by drawing a square. This shows the area the laser is going to cover when the measurements start. A green LED on the front panel shows that the laser is being initialised and goes off after the initialisation. This is very important because incomplete initialisation of the laser causes errors in the measurement process. Sometimes measurement will not even start and even if it starts, the scan action does not follow the specified position settings of the X-Y plane.

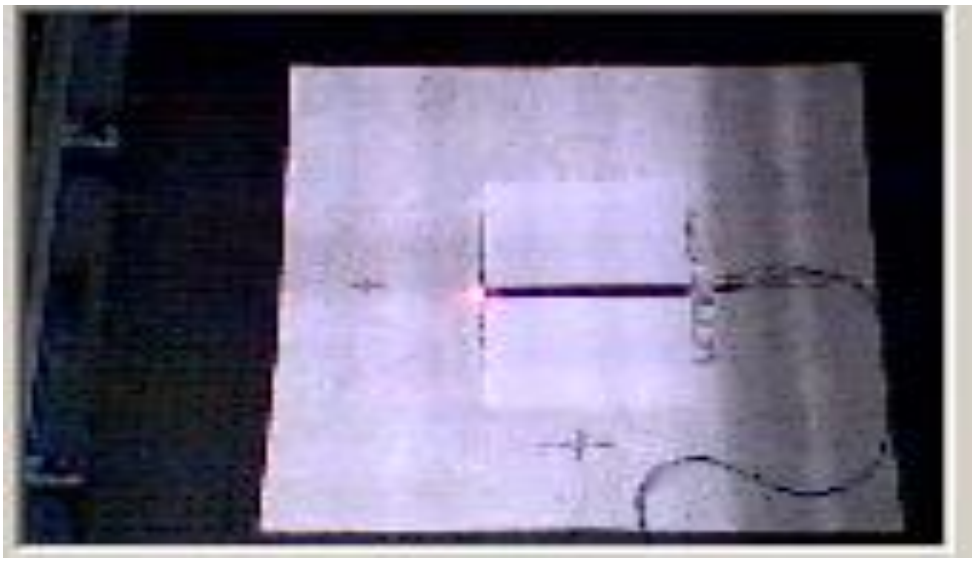

Fig 4.1 Laser position at (3500, 200) and on a cell length of nearly (20 X 1 cm)

Moreover, a successful initialisation shows that the laser will cover the cell area specified. Laser position before initialisation has been illustrated in fig.4.1 with the red spot being the laser position.

The data input section contains all the manually entered data. The entire scan action is entered through the user interface or existing files are overwritten. An error code pops up if this procedure is not done correctly. Here, the X and Y ranges are specified with the number of measurement points to be taken at each XY position and the step width with which the laser is suppose to move is also specified. Manipulation of the lock-in is possible at this stage only.

The measurement process starts after the initialisation of the laser and moves over the sample surface under investigation. This movement creates current at each point and is measured by the lock-in amplifier. The laser then jumps to the next point as specified by the data input section until measurement is complete. The current laser takes about 20 ms to stabilize after each jump and about 10 measurements are taken at each point. The average of these measurements is what is displayed as the final value on the software interface for analysis.

The final part of the system is the management of the output data. Currently, the programme only reads out the output data from the lock-in amplifier and no graphical

feedback is given. Hence the read data in the raw state is saved to file in excel when the measurement is finished.

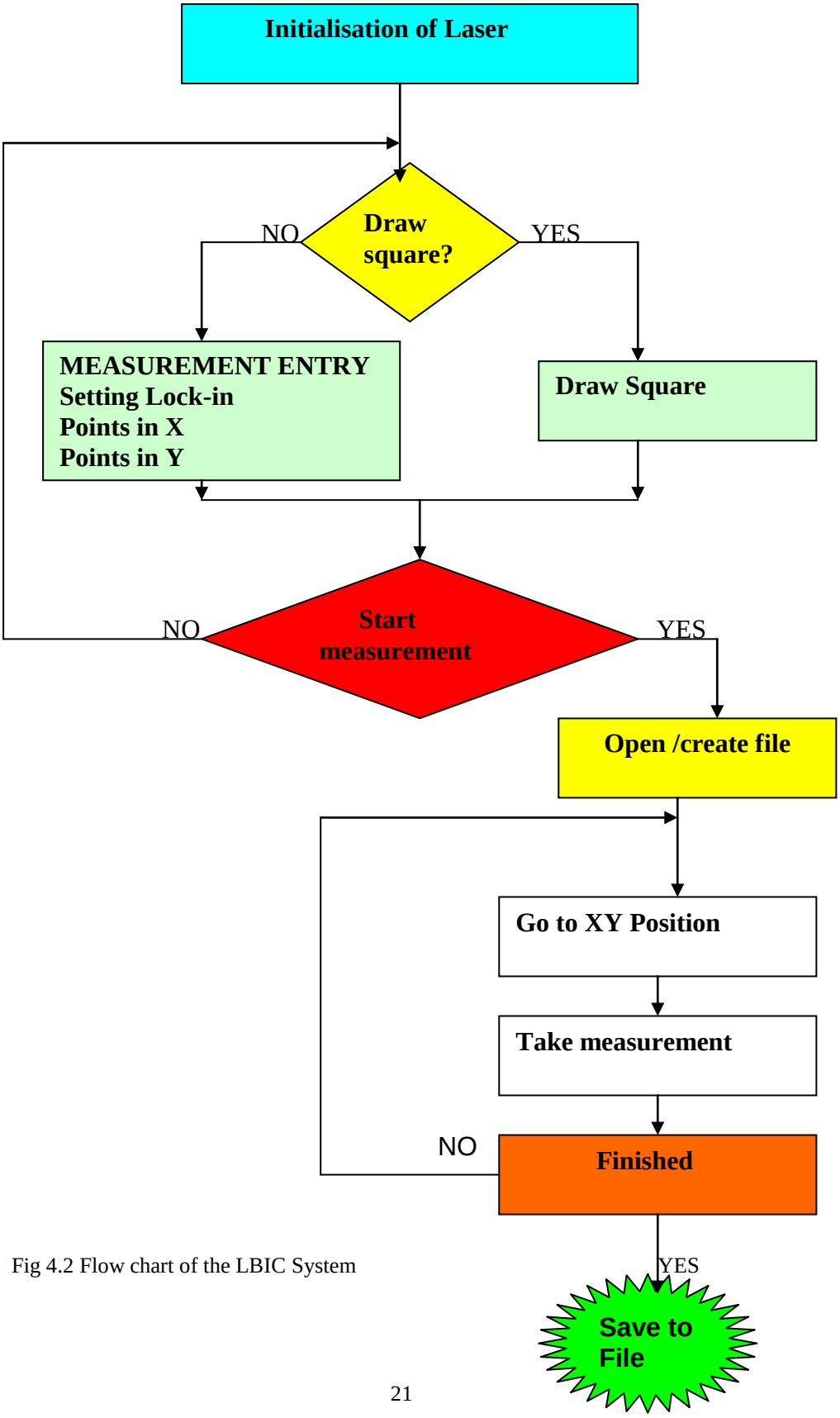

Fig 4.2 Flow chart of the LBIC System

The scanning process continues until the specified points in the X-Y directions are done.

A sample measurement taken at the first stage of the testing process with a laser settling time of about 50ms and a reference frequency of 637 Hz illustrated that various parameters need to be optimised. These measurements were taken using the standard settings (in appendix 1) and 10ms time constant, 1mV sensitivity on the lock-in amplifier.

The sampling rate for this measurement was 2.6 samples/sec which is very fast compared to Michel 2004, at 0.25 sample/s.

The time constant and the sensitivity were crucial to the accurate measurements and performance of the set up. This is depicted in fig 4.3 with a time constant of 1s.

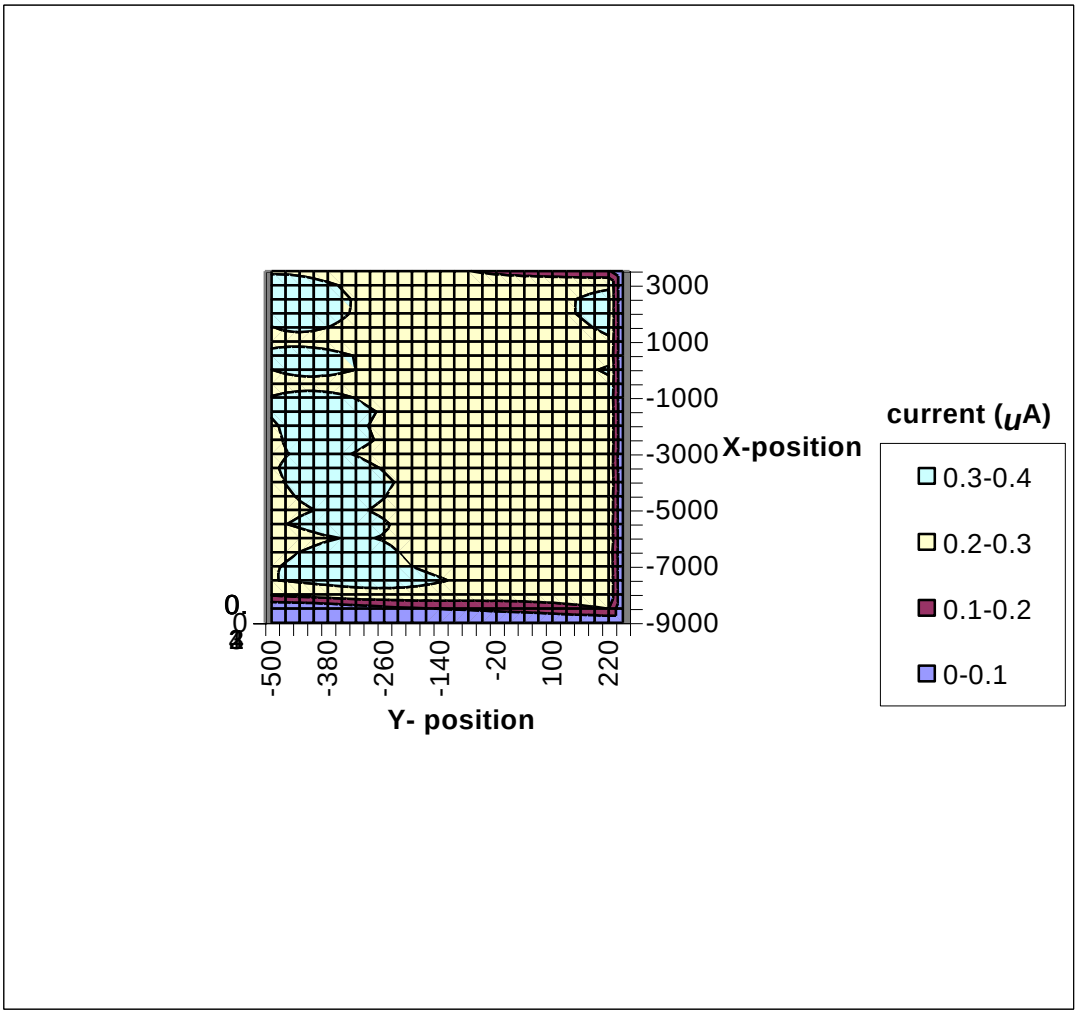

Fig 4.3. Measurement with Time constant of 1s

Figure 4.3 shows a non utilisable LBIC map and call for optimisation of the settings on the lock-in amplifier. Hence different settings such as the time constant, sensitivity and others needed improvement.

4.3 Optimisation

The settings on the lock-in amplifier are numerous. Most of these settings were not altered and were used as it is set on the lock-in amplifier as the standard settings. Setting the time constant on a lock-in sets the low pass bandwidth filter. The notion of time constant arises from the fact that a lock- in amplifier takes in an AC signal and converts it to an output DC. Therefore, a noisy input signal comes out as a noisy

output DC signal. By manipulating the time constant i.e. increasing it, the output is smoothened and can be measured accurately. The time constant therefore determines the degree of output smoothing and how slowly the output responds.

Measurements taken with the current LBIC system is shown below. The following figures shows some LBIC mapping with different time constants but same reference frequency

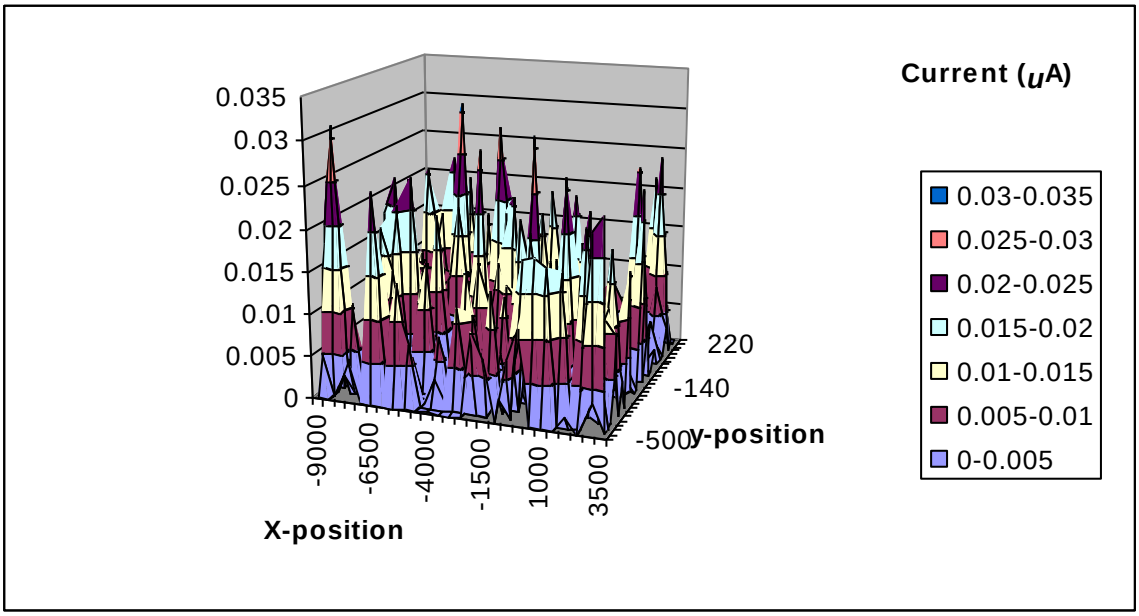

Fig 4.4 LBIC map. Time constant 10 μs / Chopper Frequency 518Hz

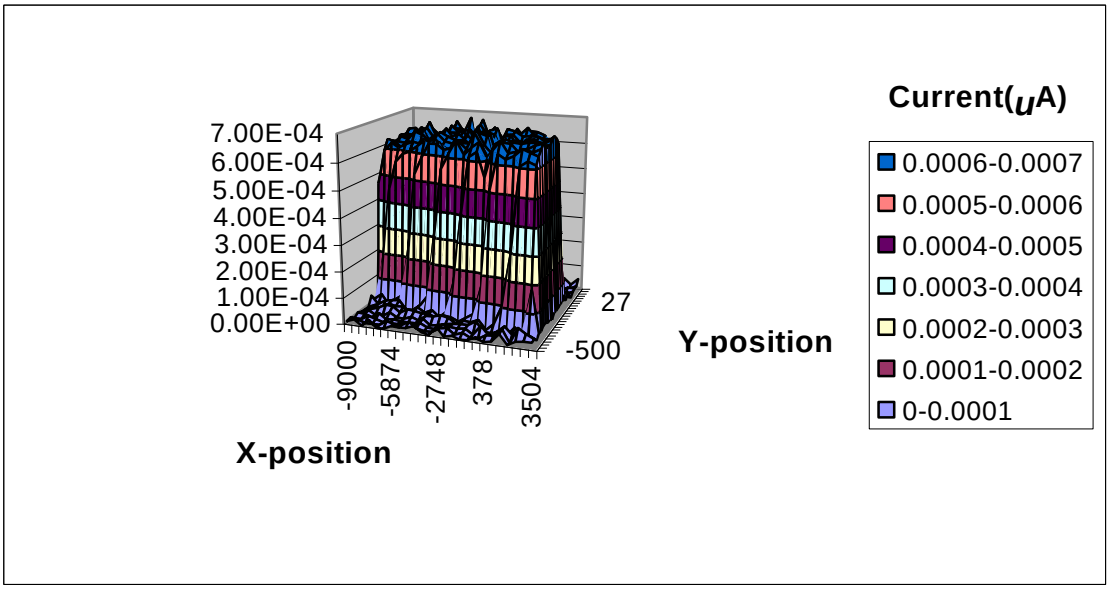

Fig 4.5 LBIC map Time constant 30ms/ Chopper Frequency 518Hz

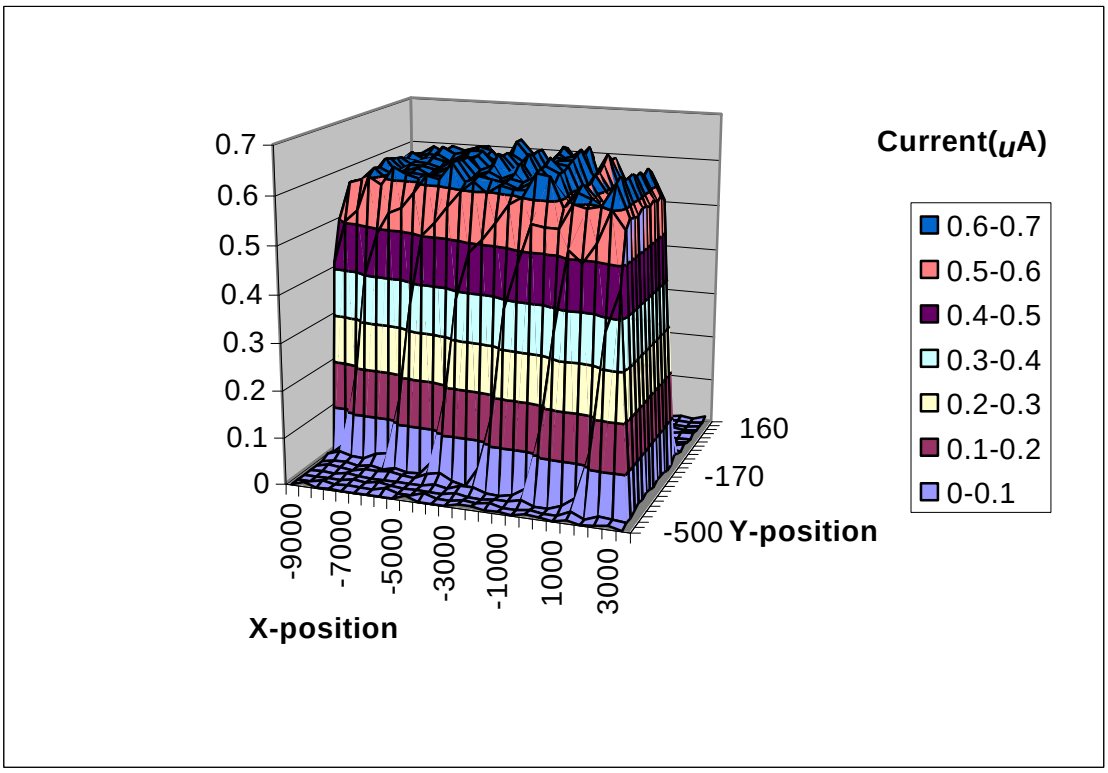

Fig 4.6 LBIC map. Time constant 100ms/chopper Frequency 518Hz

The output measurements of different time constant have been illustrated in figure 4.5-4.7. These are fast scan LBIC map of 25x 24 data points which were done within 4 minutes for one cell. The maps illustrate a good current topography at 30 and 100ms

time constant. Short time constants are responsive but rough while long time constants are smooth but sluggish. The selection of a time constants is therefore a trade off because real changes in the input signal takes many time constants to settle to a final value. These LBIC quality mapping figures can be used to understand thin film properties and also guarantee high level production quality.

The sensitivity and the chopper frequency were also investigated and the following results were achieved. As a result, this indicated that several settings needed to be altered for reliable and accurate measurements and that the same settings used for measuring current cannot be used for voltage hence a word of caution for subsequent users. These measurements were taken with 518Hz chopper frequency and 30ms time constant.

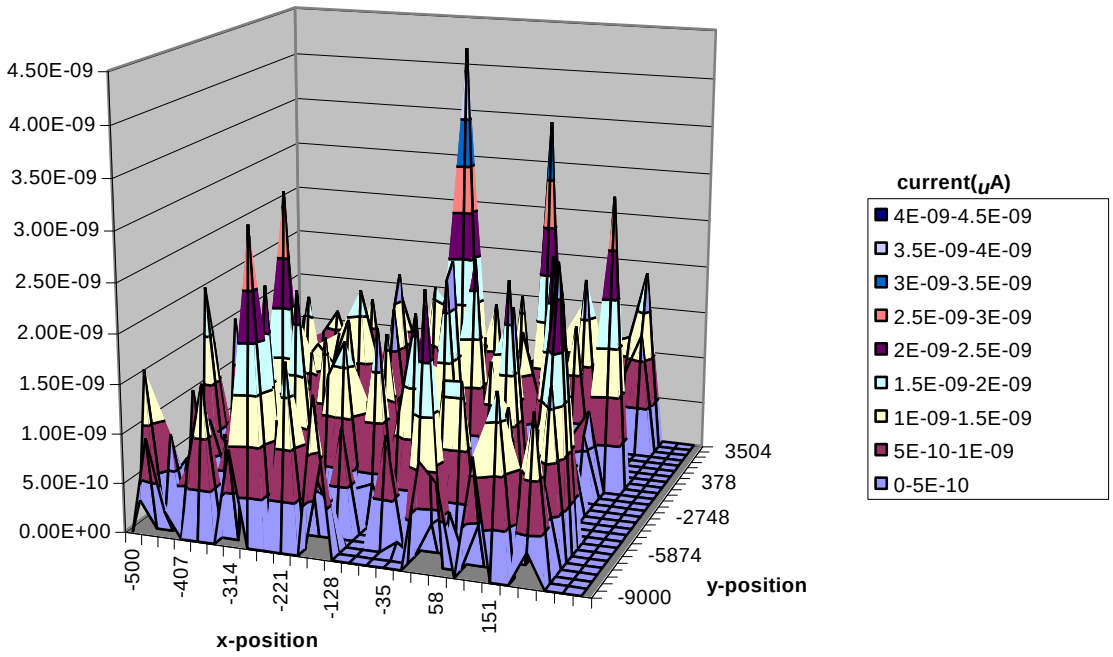

Fig. 4.7 LBIC Map Sensitivity 500nV

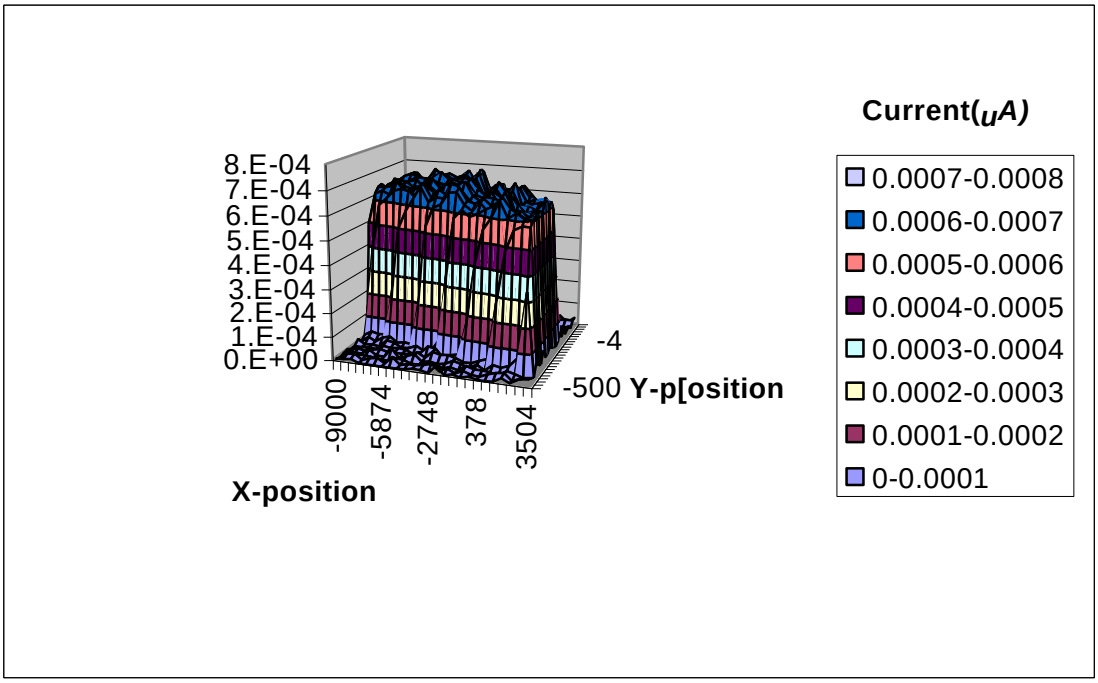

Fig 4.8 LBIC Sensitivity 100mV

Also the reference frequency was varied and graphs of their corresponding signals are plotted below. The variation is not striking as can be seen in figures 4.10 and 4.11, although it is influence by the time constant.

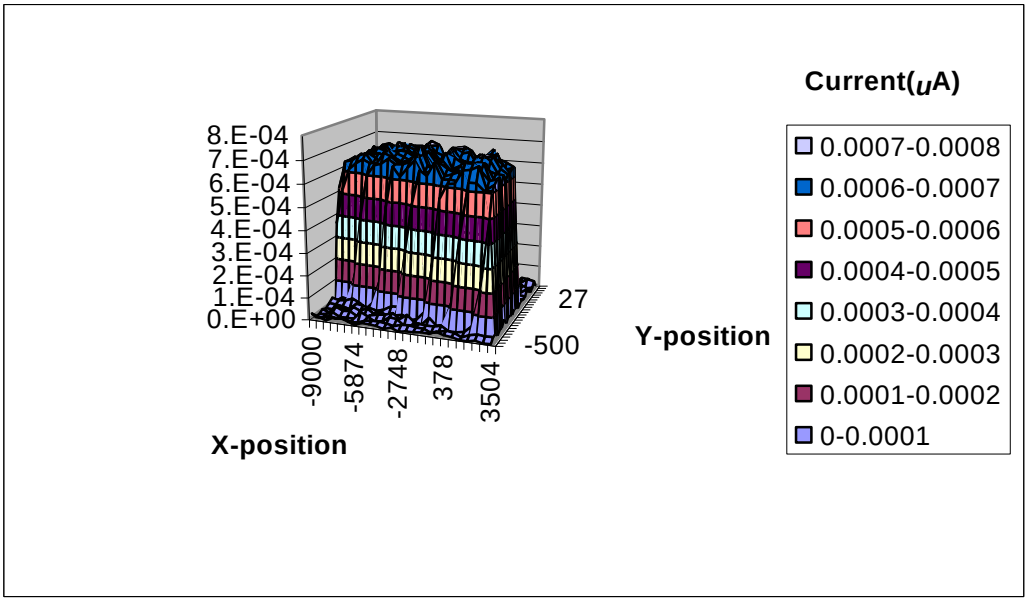

Fig. 4.9 Time constant 30ms/chopper frequency 618Hz

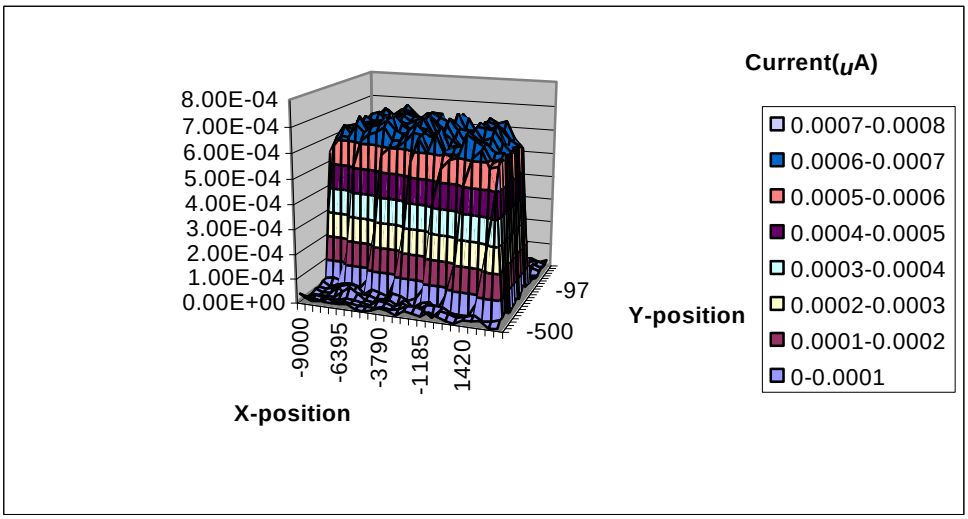

Fig.4.10. Time constant 30ms/Chopper Frequency 718Hz

4.4 Measurements across Multiple cells

At present, this technology is at the research stage in the laboratories and therefore one of the aims of this work to facilitate moving this technology to industry. This means that the current system should be able to map a whole module size of about 1.2 x 1.2m within a short time frame with a high number of cells. So far only single cells were investigated. In the following work, the number of cells will be increased and the effects on the signal strength will be demonstrated.

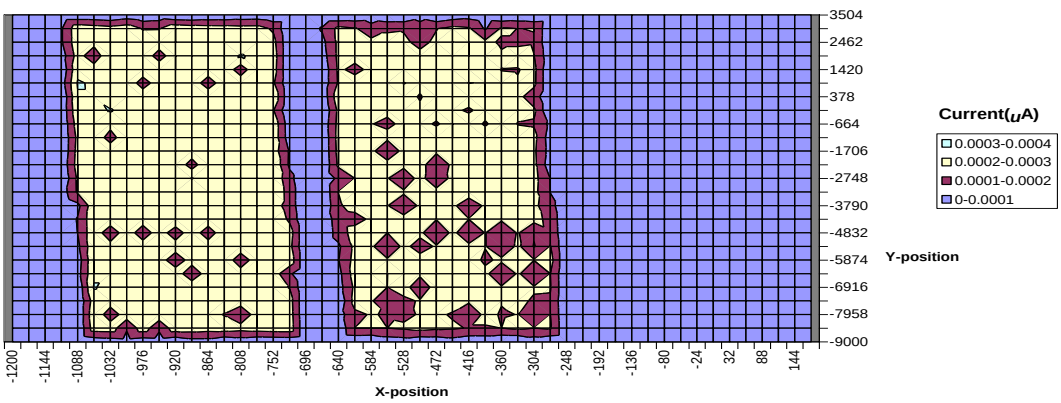

Fig 4.11. LBIC Topography of 2 cells

All the results shown so far seem promising for just a single cell, but for this technology transfer, a whole module must be mapped. The first measurement in the attempt to measure the whole module is shown in figure 4.12.

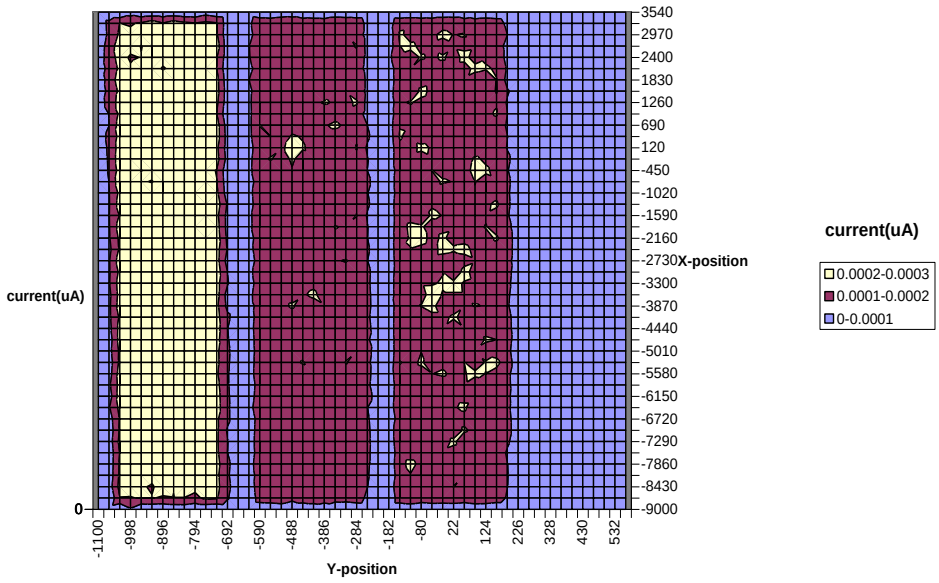

Fig. 4.12 Showing LBIC map for 3 cells.

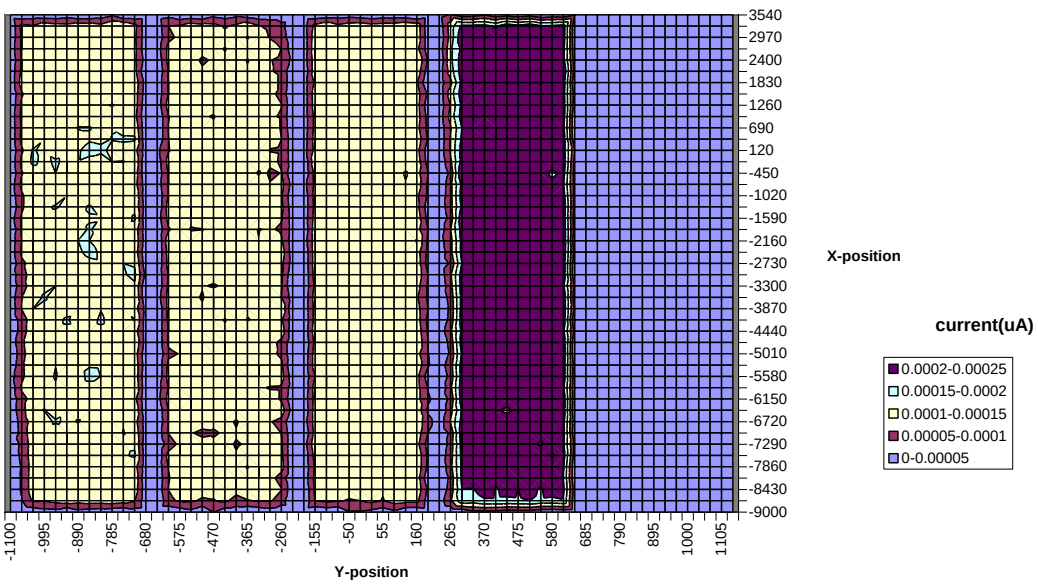

Fig 4.13 Illustrate an LBIC map for 4 cell

An optimal time constant of 30*ms* and a sensitivity of 50*mV* have been used in these current maps of up to 10 cells with a reference frequency 518Hz which is set by the

optical chopper. These are high resolution LBIC mapping and after editing it illustrate the individual cells and their current generation per laser point on the cell and can be used for detail cell evaluation.

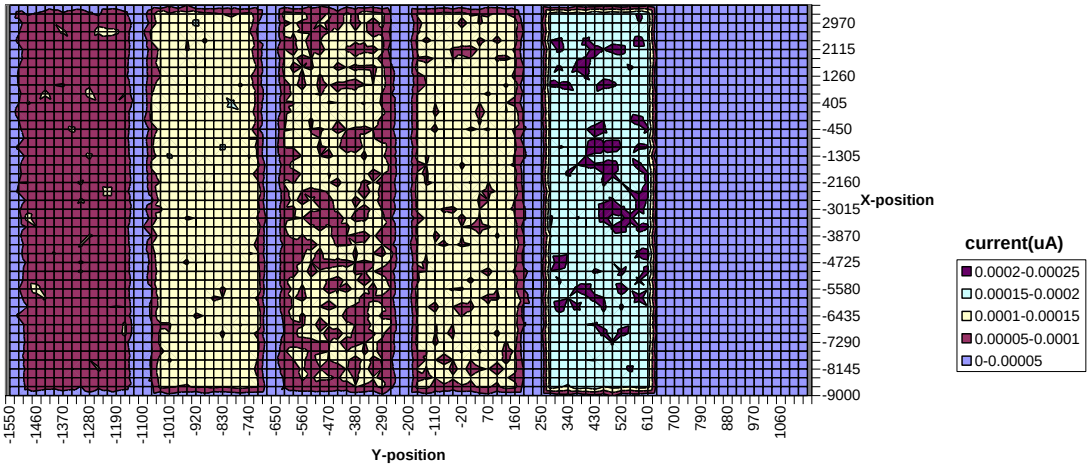

Fig 4.14 LBIC map for 5 cells

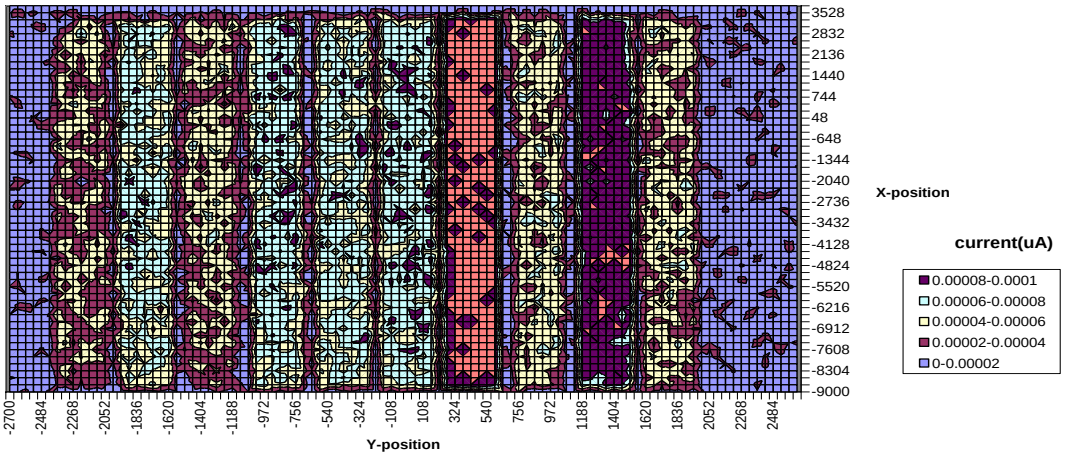

Fig 4.15 LBIC map for 10 cells

A high resolution of 1000 data points per cell of 28 X 1 cm was taken through point by point measurements over the entire cell. This took about 7 minutes for the measurement cycle which is very fast compare to a previous work which took about an hour to collect 1000 data points. But at the same time there is lots of noise that has frequency nearly the signal frequency and nearly no current is measured when the number of cells is increased further. This is evident in figure 4.15 above.

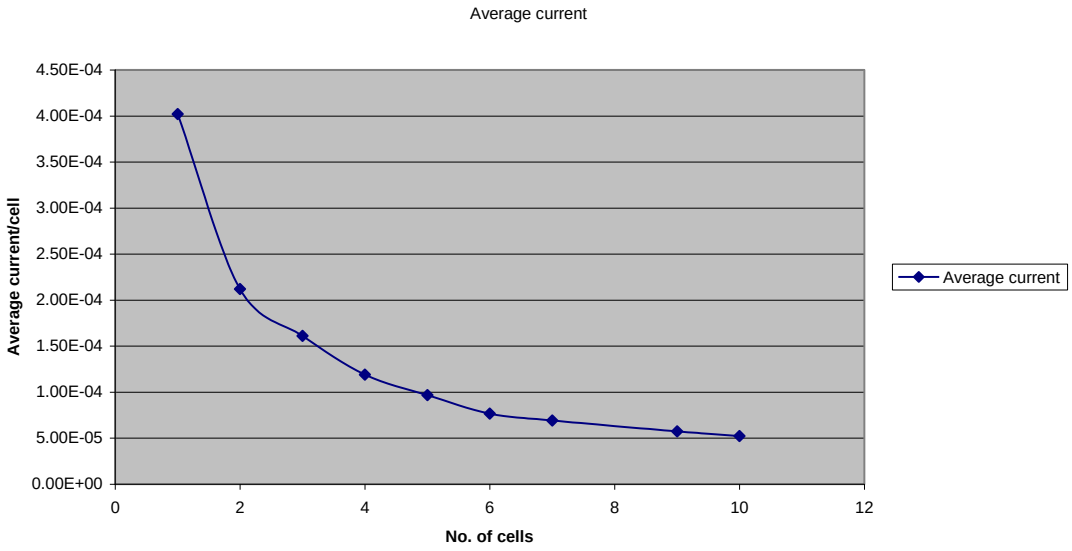

Fig 4.16 Graph of current verses number of cells

The signal is constantly decreasing and there is no significant signal for the whole module to be measured. A plot of the mean current generation versus the number of cells has been shown. This illustrates almost an exponential decline of the photocurrent current that at some time runs into the detection limits.

The LBIC system which has been programmed in LabVIEW has been tested with different settings on the lock-in amplifier such as the sensitivity, time constant and chopper frequency.

The test and modelling of the set-up shows an interesting pattern that the lock-in amplifier parameters follow and a presentation of the pattern revealed by the time constant has been shown.

First steps were taken to investigate industrially relevant test conditions by measuring multiple cell sections. Surface profiles were generated, illustrating the level of detail that is possible with this technique. Hence these results demonstrate a strong potential for industrial implementation.

CHAPTER FIVE

CONCLUSION AND RECOMMENDATIONS

Different methods exist for the quality control of solar cells ranging from solar simulator by recording the I-V curves, measurements of spectra response, and the testing of the chemical deposition with scanning electron microscope.
These tests were based on a pass or failure method and did not yield a detail evaluation of the physical properties like the LBIC system.

The LBIC system presented in this report is a prototype of an advanced measurement system with high spatial resolution for probing solar cells. This LBIC-system has been built for research and development and therefore the implementation of such device in the production line for quality control need to be studied further.
The control software which is written in LabVIEW communicates with the instruments through a GPIB bus except the laser, which is controlled by the RTC-3 board. The control system works very well but there is still research that needs to be done for further improvement. Also the control software can be improved and redefined with additional sub-VIs for setting the measurement set-up and the settings on the lock-in amplifier. The data management set- up of the system is crude and needs to be re-programmed for a better graphical representation. This can be programmed such that the software analysis the data and plot it as the measurement progresses. The current software is flexible and can be done with the help of waveform file I/O VIs and generate a 3D graph with **HIQ** in LabVIEW without going through excel which has limits to the number of data points that can be collected.

Several measurements have been taken to set the parameters on the lock-in amplifier as one of the major problems in the present set-up. The time constant was one of the settings on the lock-in that was optimised. It was realised that the time constant varies as the sensitivity is changed and this variation, also depends on the reference frequency. This accuracy of measurement versus time constant is an estimate because quality change could not be quantified. This is important because it decides how long

an experiment should take and therefore a trade-off is needed. This is achieved for specific sensitivity. Fixing the time constant and reference frequency but varying the sensitivity reveals similar characteristics which made the lock-in amplifier very versatile.

Optimal settings of 30ms time constant and 50mV sensitivity were used as the settings for all measurements. The reference frequency did not change the quality of measurement significantly and was fixed at 518Hz. These entire tests were carried out for a single cell with the homogenous background illumination of the halogen lambs.

The laser works quite well but there is the need for further improvement on the settling time although that will have influence on the fastness of the measuring system. Currently the laser does not understand the command when it gets to the Y-range with negative start and stop and this will need a bit of programming to fix it.

The transfer of this system to industry is only possible when the system can map a whole module. The system has been used successfully to map up to 10 cells with very high accuracy and resolution of 2.5 points per mm with an average speed of about 2.6 points per second. But due to the decreasing nature of the cell current as the number of cells increases, a significant signal can not be measured after this stage. This is the case and therefore the whole module has been mapped in bits up to ten cells maximum. The signal generated is high enough to do current mapping for these multiple cells. This has been the step forward so far for moving the system into industry.

This low signal can be improved in the future by including a pre-amplifier before the signal goes to the lock-in amplifier. Although there has been an improvement, further optimisation can enhance the system performance. This system is still slow compare to Agostinelli et al [2001] which map an array of 30 X 30 points in less than 3 seconds. But this can be explained by the fact that 10 measurements are taking at each point at the present system.

Laser beam induced current technique is the device the photovoltaic industry needs to be able to identify and follow the various steps for any variation in the final product. This is due to its non-destructive nature with very good spatial resolution to

characterised electrical performance of solar cell and photosensitive devices qualitatively and quantitatively.

Spatially limited problems of solar cells can be revealed by using the current LBIC system. This high resolution maps can be used to identify faults in photosensitive devices and would help in the quality assessment in the production line. This kind of analysis would provide a tool for improving the cell efficiency and help in the mass production to reduce the cost of cells.

The state of the experimental set-up and the control system have been improved significantly. Different parts of the set-up can be optimised for a better and fast scanning and also there is (more) room for improvement of the whole measurement process.

This work has demonstrated clearly that the LBIC system is a viable technology for an inline quality assessment of solar cell production and is possible to move this technology to industry but there is still some work to be done to achieve this. The scanning rate has been improved and an optimal time constant has been achieved for specific sensitivity but there are still lots of settings on the Lock-in amplifier that could be optimised for better measurement. Several attempts made to scan the whole module failed due to low signal from the cells. However, a systematic research with solar cells from different manufacturers should be performed. This should further elucidate the potential of LBIC as a non-destructive in-line characterisation technique. More importantly this will allow the solar PV industry to move forward in terms of efficiency and cost effectiveness.

REFERENCES

Acciarri,M., Binetti, S., Garavaglia, M., and Pizzini, S. (1996) Detection of junction failures and other defects in silicon and III-V devices using LBIC technique in lateral configuration. Material science and Engineering. B42, 208-212

Acciarri, M., Binetti, S., Racz, A., Pizzini, S., and Agostinelli, G (2002). "Fast LBIC in-line characterization for process control in the photovoltaic industry". 17th European photovoltaic solar energy conference.

Agostinelli, G., Friesen, G., Merli, F., and Dunlop, E.D. (2001). Large area photocurrent maps for Routine PV module inspection. Proceedings of the 17th European photovoltaic solar energy conference.

Bishop H. R. (2004) "Learning with LabVIEW 7 express" Pearson Prentice Hall, NJ, ISBN: 0-13-117605-6

Delahoy, A.E. and Payne A.M. (1997). Determination of the internal series resistance of CIS and CIGS Photovoltaic cell structures. Proceedings of the 25th IEEE PVSC

Dunlop, E.D., Zaaiman, W., Ossenbrink, H.A., and Helmke, C. (1997) Towards a stable standard reference device for the measurement and monitoring of Amorphous silicon modules and arrays. 14th ECPVSEC, Barcelona, Spain. pp1632-1635.

Galloway, S. A. (1996) Microscopic characterization of Cds/CdTe thin film Photovoltaic devices using scanning optical and electron beam injection technique. "Proceedings of the 13th Euro. PVSC 2072 (1995)

Kress, A., Pernau, T., Faith,P. and Bucher, E. (2000) LBIC measurements on low cost back contact solar cells. Universitat Konstanz, Fachbereich Physik, Germany.

Markvart, T. (1997) Solar Electricity. John Wiley & Sons, New York, USA, ISBN: 0-471-98852-9

McMahon,T.J., and Roedern, B.V. (1997) Effect of light intensity of current collection in thin film solar cells. Proceedings of the 26th IEEE PVSC 377 (1997)

Michel, T. (2004) "Design and construction of LBIC measurement system for Photovoltaic Application", Diplomarbeit thesis, Loughborough University, CREST. United Kingdom.

Rezek, B., Nebel, C.E and Stutzmann, M. (2002). LBIC in polycrystalline silicon thin films prepared by interference laser crystallisation. Journal of Applied physics. Vol. 91 No. 7

Schultz, O. (2004) Thermal oxidation processes for high-efficiency multicrystalline silicon solar cell. 19th European Photovoltaic solar energy conference, 7-11 June. Paris.

Travis, J., and Wells, L. (2002) LabVIEW for everyone. Prentice Hall PTR, N.J, ISBN: 013065096x

Vorasayan, P. (2004) Realistic energy yield of different photovoltaic technologies in Loughborough. Master thesis. Loughborough University, CREST United Kingdom.

Zweibel, K. (1990) Harnessing Solar power: The photovoltaic challenge". Plenum Publishing corporation, New York, USA, ISBN: 0-306-43564-0

APPENDIX

STANDARD SETTINDS ON LOCK-IN AMPLIFIER AND GRAPHS

REFERENCE / PHASE

Phase	0.000°
Reference Source	Internal
Harmonic #	1
Sine Amplitude	1.000 Vrms
Internal Frequency	1.000 kHz
Ext Reference Trigger	Sine

INPUT / FILTERS

Source	A
Grounding	Float
Coupling	AC
Line Notches	Out

GAIN / TC

Sensitivity	1 V
Reserve	Low Noise
Time Constant	100 ms
Filter dB/oct.	12 dB
Synchronous	Off

DISPLAY

CH1	X
CH2	Y
Ratio	None
Reference	Frequency

OUTPUT / OFFSET

CH1 Output	X
CH2 Output	Y
All Offsets	0.00%
All Expands	1

AUX OUTPUTS

All Output Voltages	0.000 V

SETUP

Output To	GPIB
GPIB Address	8
RS232 Baud Rate	9600
Parity	None
Key Click	On
Alarms	On
Override Remote	On

DATA STORAGE

Sample Rate	1 Hz
Scan Mode	Loop
Trigger Starts	No

STATUS ENABLE REGISTERS Cleared

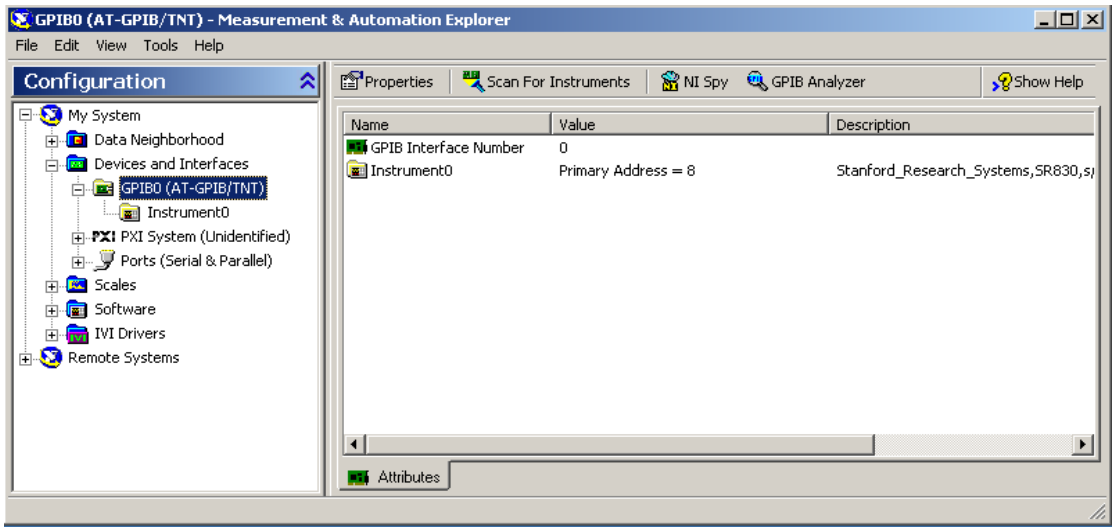

Screen snapshot illustrating MAX identification of instruments

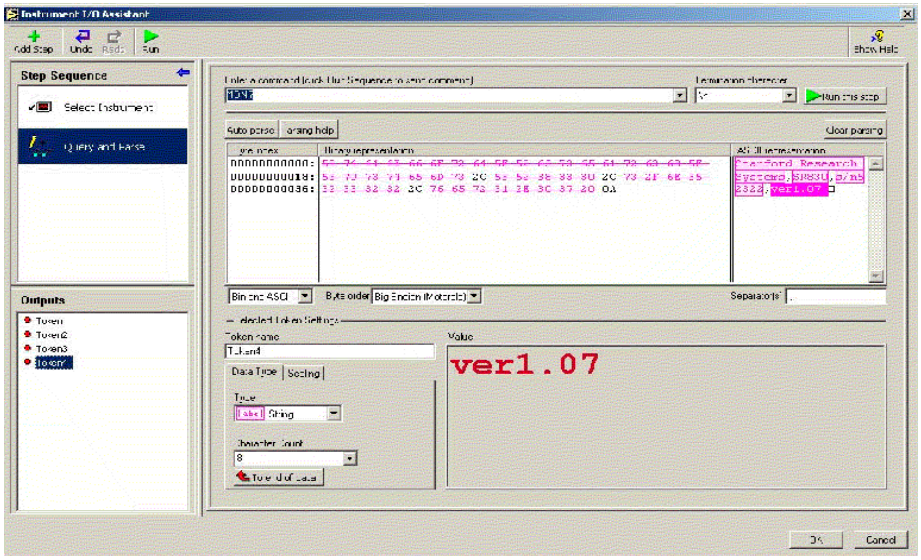

Instrument I/O assistant

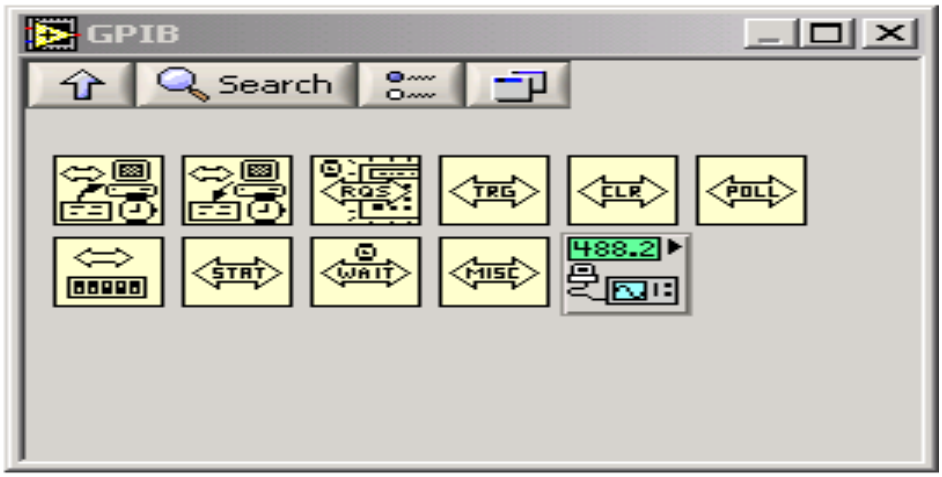

Fig 3.4 Showing a GPIB driver Palette

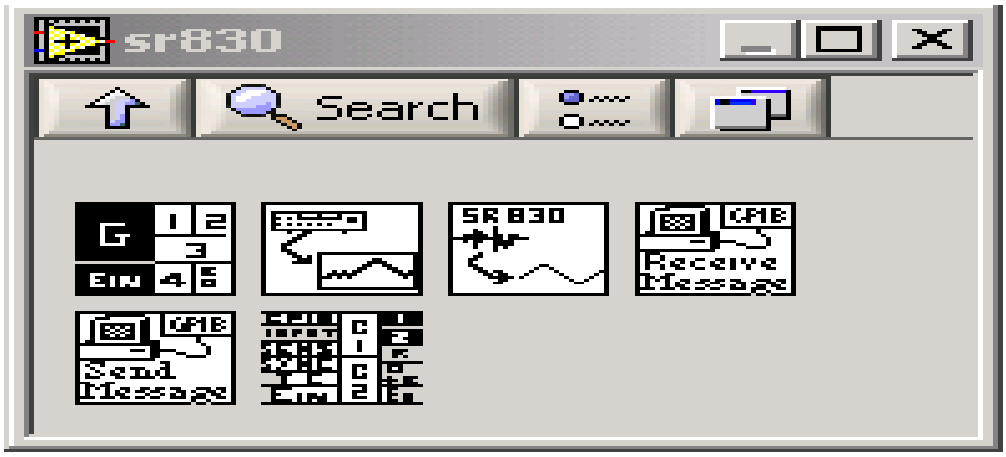

Fig 3.5 showing SR 830 driver Palette

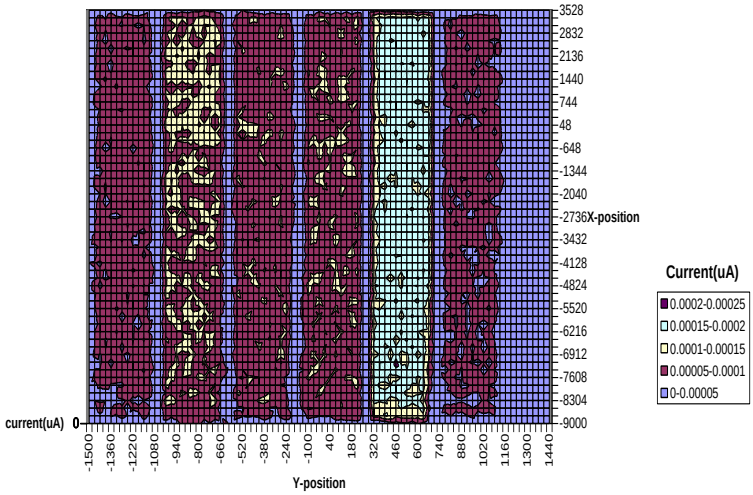

LBIC map for 6 cells

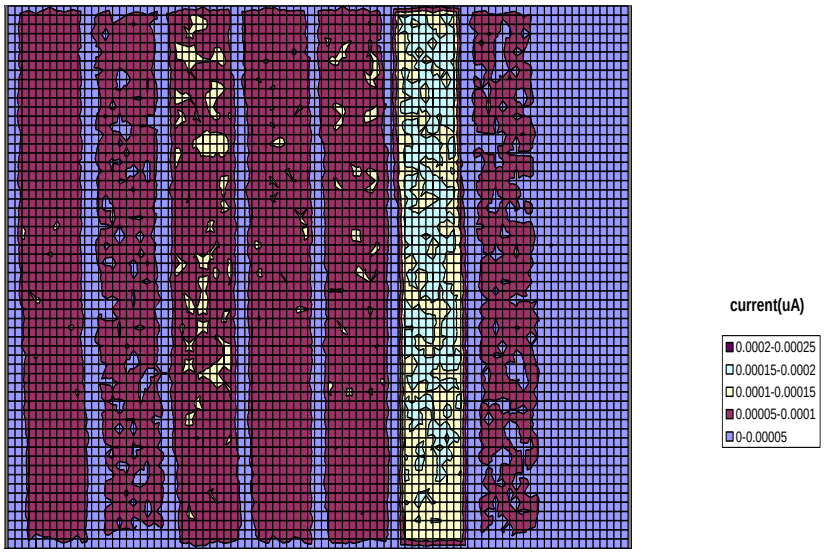

LBIC map for 7cells

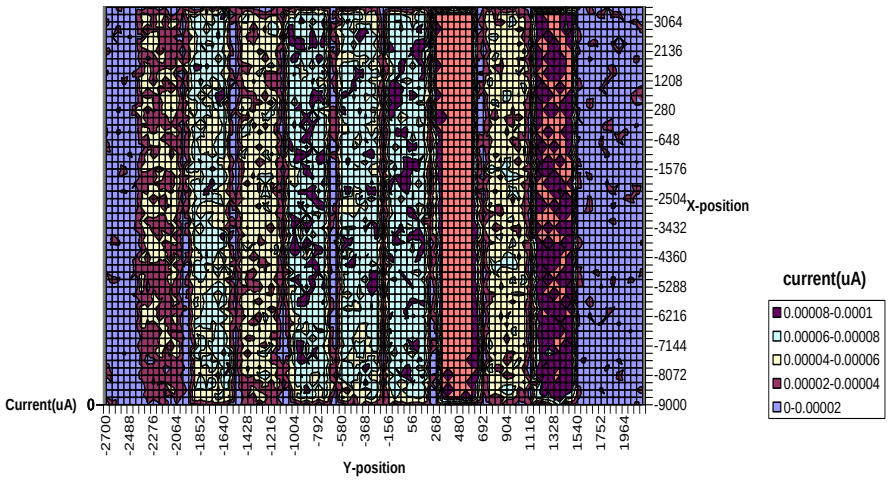

LBIC map for 9 cells